Arch. Metall. Mater. **65** (2020), 1, 417-422

DOI: 10.24425/amm.2020.131744

D. NIEMIEC[1*], M. MIKUŚKIEWICZ[1*]

EFFECT OF ULTRASONIC-ASSISTED PREPARATION OF POWDERS ON SYNTHESIS OF RARE EARTH ZIRCONATES

The aim of the research was to determine the effect of sonochemical treatments on homogenization of powders as well as phase composition and thermal stability of sinters. The compounds were prepared from Eu_2O_3 and ZrO_2 powders, weighed in the mass ratio 1:1. Initially ultrasound treatment was applied. 750-Watt ultrasonic processor VCX-750 equipped with sealed converter VC-334 and horn 630-0219 with the diameter of 13 mm (Sonics & Materials, Inc.) was used as a source of ultrasound. Applied ultrasound frequency was 20 kHz, power density was controlled in the range from 75 W/cm^2 to 340 W/cm^2. Investigated compounds were synthesized via solid-state reaction (SSR). The Differential Scanning Calorimetry (DSC) was used in order to investigate the effect of sonochemical treatment on the synthesis of prepared mixtures the powders particle size distribution was analyzed. Ultrasound treatment what wasn't never been reported before.

Keywords: pirochlore, ultrasonic, TBC

1. Introduction

Thermal barrier coatings (TBC) are multi-layer coating systems used in aviation and power engineering. Particularly, they are embedded with combustion lines, blades and other elements in the so-called hot zone for thermal insulation and protection of the substrate against hot and corrosive gas streams [1-4]. Turbines covered with the TBC system are exposed to extremely harmful conditions, which include high mechanical stress at elevated temperature, thermal fatigue and the occurrence of molten deposits resulting from the combustion of low-quality fuels and the presence of foreign particles in the air [4-6]. Melting pollutants of the environment (dust, sand, volcanic ash and runway residues) are known as CMAS (calcium-magnesium-aluminum silicate), these impurities cause a reduction in the durability and thermomechanical properties of the coating through erosive wear and blocking of cooling holes [7-10]. The most important factor affecting the lifespan of TBC systems is the hot corrosion caused by molten sodium sulphate and vanadium oxides which are fuel contaminants [11-13]. Due to numerous requirements such as high melting point, no phase transitions between working temperature and room temperature, very low thermal conductivity, chemical resistance, thermal expansion coefficient close to the metal substrate, good adhesion to the substrate and low sintering rate of the porous microstructure number possible materials that may be applicable are limited.

The most commonly used material for the outer insulation layer is zirconium oxide doped with 7-8% by weight. Yttrium oxide. However, phase stability and sintering resistance limits the increase in temperature at the turbine inlet. For this reason, a lot of efforts have recently been made to find new insulating materials for the external value. In recent years, the greatest interest has been gained by zirconates of rare earth elements with the general formula $RE_2Zr_2O_7$ and pyrochlore structure as a promising candidate in application on TBC [14-15].

The stability of the P-type structure is mainly determined by the coefficient of cation radiations (rA / rB). The structure of pyrochlore is stable when the value of rA / rB is in the range of 1.48-1.76. In addition, the ordering of the structure depends on the stoichiometry and the thermal history of the material [16-17]. Ceramics with a pyrochlonic structure of the general formula $A_2B_2O_7$ (where site A is occupied by a larger cation 3+, and place B by a cation smaller 4+) is a material of high scientific and technological importance. Representatives of this group of materials proposed as candidates for the external insulation layer are zirconates, ceranium and hafnium of rare earth metals. These materials are characterized by improved thermal properties

[1] SILESIAN UNIVERSITY OF TECHNOLOGY, 8 KRASIŃSKIEGO STR., 40-019 KATOWICE, POLAND

* Corresponding authors: dawid.niemiec@polsl.pl, marta.mikuskiewicz@polsl.pl

compared to yttrium-stabilized zirconium. Therefore, they are interesting materials for the insulation layer at TBC.

The basic methods of powder synthesis are solid state reactions and various types of wet chemical methods. In order to increase the efficiency of synthesis, the use of ultrasound was proposed. In this method, strong ultrasound (sound over 20 kHz) is used to simulate chemical reactions and physical changes in the liquid. These effects arise as a result of acoustic cavitation. Ultrasonic radiation can be used at room temperature and at ambient pressure to promote heterogeneous reactions that only occur under extreme pressure and temperature conditions. The acoustic pressure wave consists of alternating tribulations and rare phenomena in the transmitting medium along the wave propagation direction. When high vacuum is applied to liquids, the intermolecular van der Waals forces are not strong enough to maintain cohesiveness and small cavities (also known as cavitation bubbles) or microbubbles filled with gas are formed. Cavitation bubbles exist only in several acoustic cycles. At this time, the bubbles grow during the expansion phase of the ultrasound wave, then shrink and the bubble burst violently. In the last phase, very high temperature and pressure arise. The theory of cavitation of thermal "hot spots" assumes that short-lived, localized hot spots form in liquids. It turned out that the effective temperature of the resulting transient local "hot spots" is in the range of 520 ± 650 K. Assuming this value, the pressure during collapse would be about 1700 atm. In addition, bubble persistence is less than a microsecond, while the cooling / heating rate is over 109 K/s [18]. In the case of liquid-solid systems, the liquid stream is generated by the collapse of bubbles. If the collapse takes place close to the solid surface, the rapid liquid streams can be driven into the surface of the particle. Shock waves can cause removal of the surface coating, generate localized high temperatures and pressures and improve the transfer of liquid-solid mass [19]. The aim of the study is to check if the sonochemistry process will facilitate homogenization of zirconium powders of rare earth elements, which can potentially be used as an insulating layer in coating thermal barriers.

2. Experiment description

The compound was prepared from the constituents (Eu_2O_3 and ZrO_2), weighed in the mass ratio 1:1. In a typical procedure, the mixture of e.g. 2.650 g Eu_2O_3 and 2.650 g ZrO_2 The powders were mechanically ground up using a mortar. Then they were poured into a beaker containing was immersed at room temperature in 18 ml absolute ethanol, which was contained in polypropylene container. As a source of ultrasound 750Watt ultrasonic processor VCX-750 equipped with sealed converter VC-334 and horn 630-0219 with the diameter of 13 mm (Sonics & Materials, Inc.) was used. The end of horn was placed inside of container and was submerged in liquid. In this way large energy of ultrasound can be delivered directly to the reaction mixture. Ultrasound frequency was 20 kHz and power density was con-

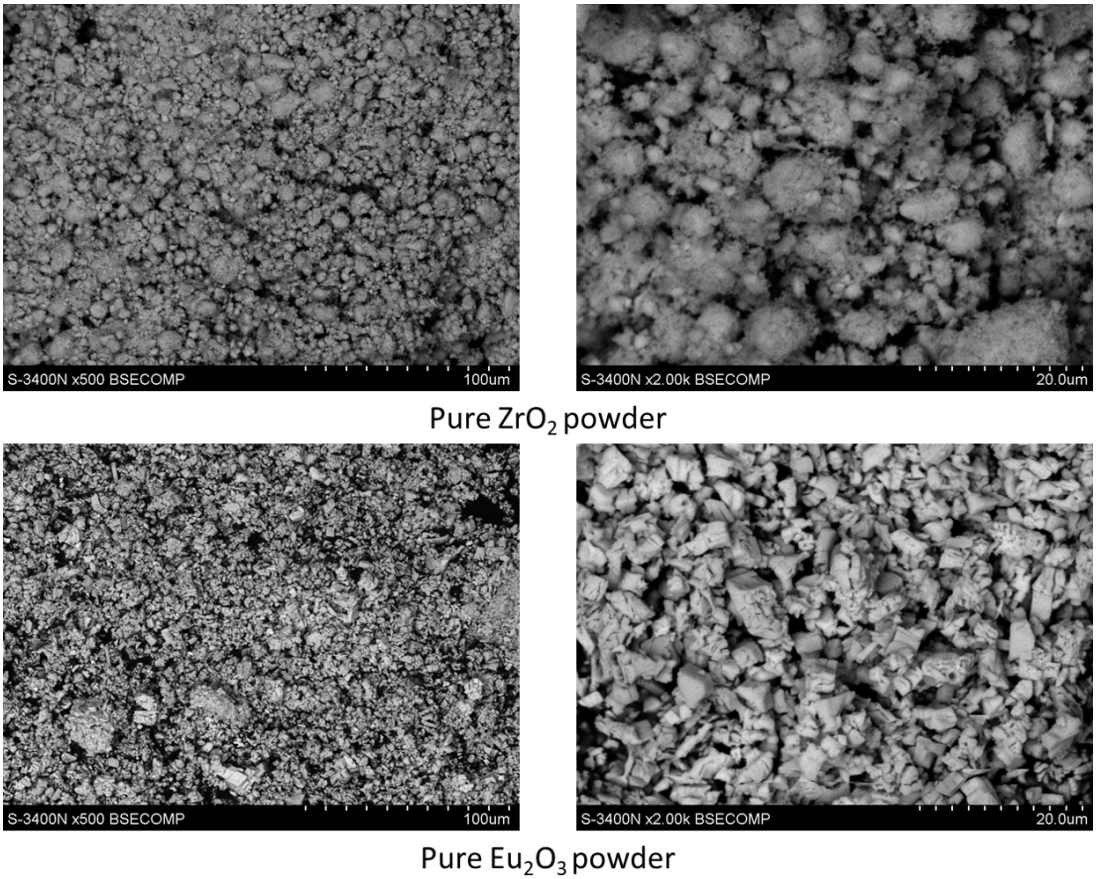

Fig. 1. Morphology of pure powders

trolled in the range from 75 W/cm^2 to 340 W/cm^2. A reaction cylinder was kept in constant temperature (293 K) during the whole synthesis by immersion it in water bath whose temperature was stabilized by refrigerated circulating bath AD07R (PolyScience). The time of sonification was always 3 h.

Grain analysis was performed using a Malvern Mastersizer 3000 laser particle analyzer for a pure mixture of powders and mixtures subjected to sonochemistry. XRD phase composition analysis was performed using JEOL JDX-7S X-ray diffractometer. The Hitachi 4200 scanning microscope was used to evaluate the morphology of the powders. To observe the thermal reactions, DSC analysis was performed using the Netzsch DSC 404 F1 Pegasus differential scanning calorimeter. The test was carried out at room temperature up to 1400°C at a heating rate of 5°C/min in argon atmosphere

3. Results

At the beginning, four blends of powders were made in a 1:1 mass fraction of ZrO_2 powder and Eu_2O_3 powder. Then one was homogenized in an agate mortar in ethyl alcohol for 10 min. The other three mixtures were subjected to sonochemical homogenization in alcohol with 150 W, 300 W and 450 W respectively. Figure 1 shows the morphology of the starting powders. The ZrO2 powder has a globular shape and shows a tendency to coagulate whereas the Eu2O3 powder has a polyhedral shape. Phase analysis (Fig. 2) revealed the presence of ZrO_2 (card no. 37-1484) in the monoclinic phase whereas in the initial powder Eu_2O_3 they occur in the dominant phase of cubic (card no. 34-0392) and monoclinic (card no. 71-0589). The morphology of the mixed powders is shown in Figure 3. Sonochemical treatment results in the formation of powder conglomerates. The greater the power delivered during the homogenization process, the larger conglomerates are formed.

Figure 4 presents the distribution of grain analysis for the starting powders ZrO_2 and Eu_2O_3 in comparison to the mixture of powders obtained in mortar and alcohol. Eu_2O_3 powder is more homogeneous if the particle size in comparison to ZrO_2 powder as shown by grain analysis. The grain analysis of the blends produced (Fig. 5) shows the influence of sonochemistry on the higher proportion of fine particles compared to traditional mortar grinding as well as the formation of a particularly large proportion of coagulated particles in the variant 4. The D-values chart summarizes data for ZrO_2 (1), Eu_2O_3 (2) starting powders and mixtures obtained in a mortar and alcohol (3), in 150W (4), 300W (5) and 450 (6) ultrasounds (Fig. 4).

In the grain distribution graphs, the occurrence of 1000 μm particles resulting from the phenomenon of coagulation can be observed. Such particles are noticeable in the case of coarse ZrO_2

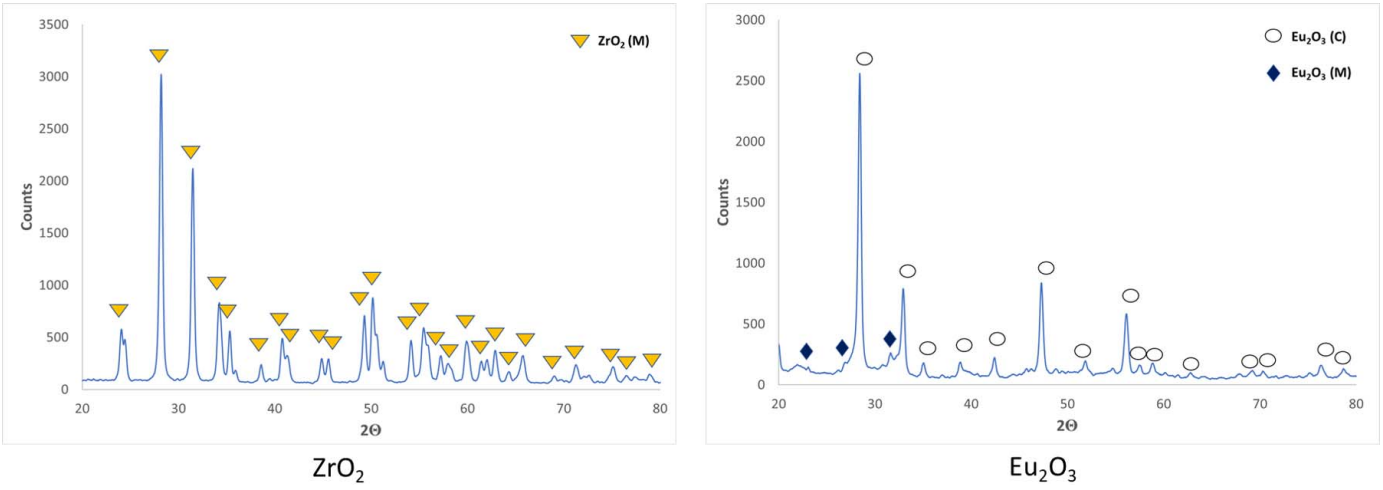

ZrO_2 Eu_2O_3

Fig. 2. XRD patterns of pure powders

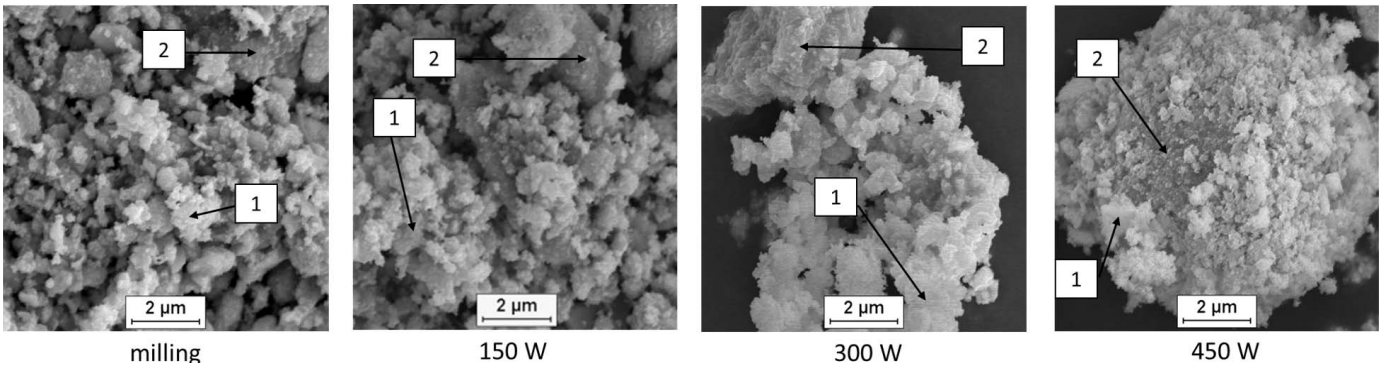

milling 150 W 300 W 450 W

Fig. 3. Morphology of powder mixtures after different types of homogenization

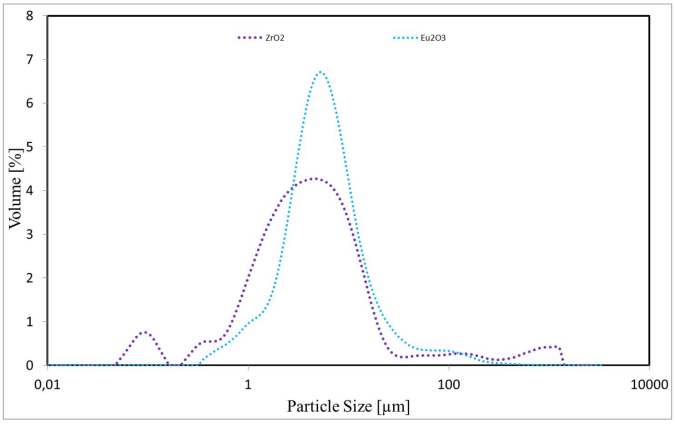

Fig. 4. Graph of particle size distribution of pure powders

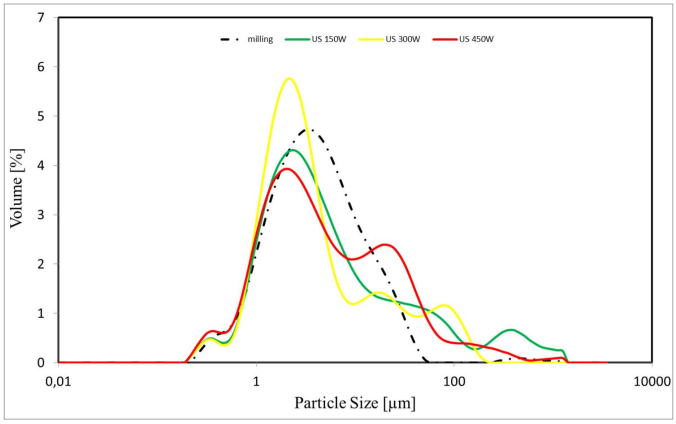

Fig. 5. Graph of particle size distribution

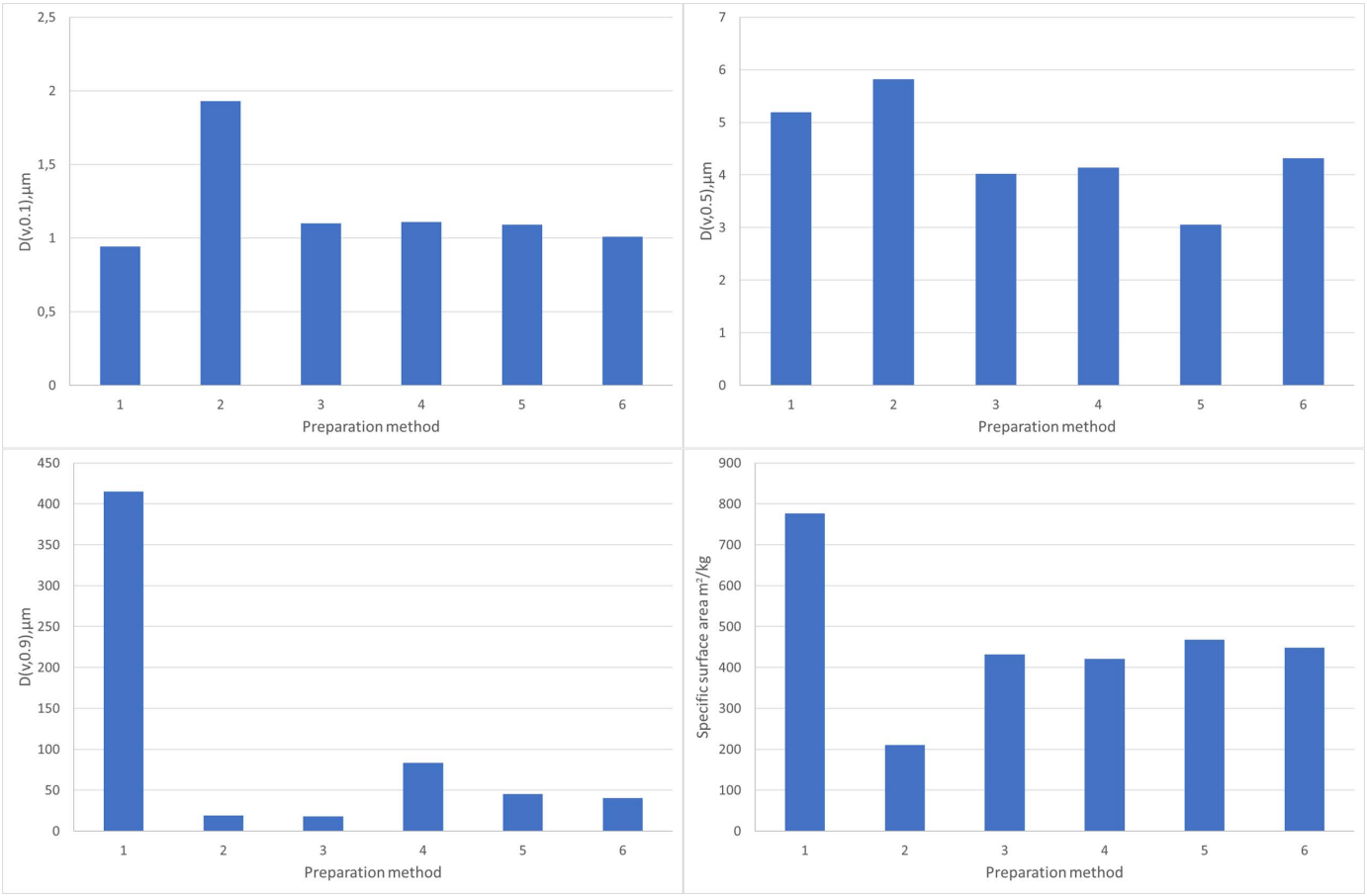

Fig. 6. Graph of D-values

powder as well as in the case of mixed powders subjected to the sonochemistry of 150W and 450W. The sonochemistry process promotes division into a larger number of powder fractions and the formation of numerous coagulated particles formed as a result of the interaction of a high energy.

Figure 7 presents the results of calorimetric tests. In the pure ZrO_2 powder, when heated at 1175°C, the transformation from monoclinic to tetragonal (1) takes place, while during cooling at 1035°C the inverse transformation (2) takes place. In the case of Eu_2O_3, during heating in 285°C, dehydration occurs (3), while at 1100°C the conversion from the cubic structure to monoclinic occurs (4). During cooling there is no reverse transformation. In the case of a mixed mixture in a mortar there is dehydration (5) in 1145°C the transformation of Eu_2O_3 from cubic to monoclinic (6) takes place. For the mixture subjected to sonochemistry with the power of 150 W, a stronger dehydration effect (7) and the Eu_2O_3 transformation (8) are observed. In the sample subjected to 300 W sonochemistry homogenization during the heating process, the dehydration process (9) takes place at 1145 and the conversion of Eu_2O_3 from cubic to monoclinic (10) takes place. During the heating of the 450W ultrasound powder, the dehydration effect (11) appeared at a temperature of 320°C.

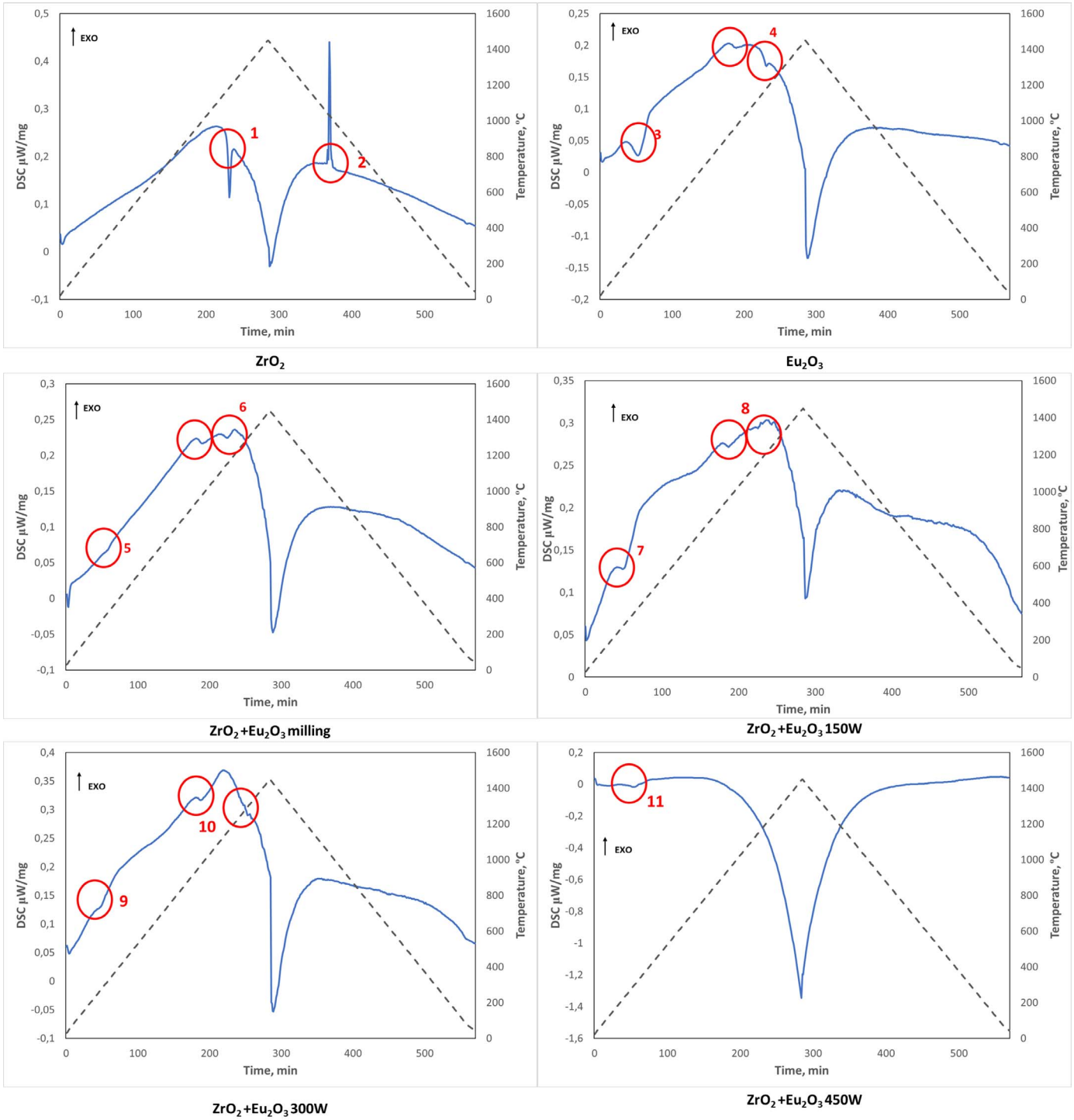

Fig. 7. DSC curves of ZrO_2-Eu_2O_3 powder mixtures

The obtained four variants of powder blends were sintered at 1300°C for 2 hours at 15 MPa. The resulting sinters were then subjected to X-ray diffraction. The results of the phase composition test are shown in Figure 8. The phase analysis of the sinter obtained from the mixed powder in the mortar showed the presence of the following phases: $Eu_2Zr_2O_7$ (card no. 24-0418) with a pyrochlore structure, two phases with fluorite structure $Eu_{0,2}Zr_{0,8}O_{1,9}$ (card no. 71-1303), $Eu_{0,5}Zr_{0,5}O_{1,75}$ (card no. 78-1292) and the occurrence of small reflections corresponding to the phases of the right powders monoclinic ZrO_2 (card no. 37-1484), Eu_2O_3 with a structure cubic (card no. 34-0392) and monoclinic Eu_2O_3 (card no 71-0589). There were also small reflections, which are difficult to assign a specific phase. In the case of sinters obtained from sonochemically homogenised powders with the power of 150 W and 300 W, the predominant phase is $Eu_2Zr_2O_7$ with a pyrochlore structure, there are also small reflections of Eu_2O_3 cubic structure, especially in the case of sintered powder obtained with the sonochemical method of 300 W, reflections of the $Eu_{0,2}Zr_{0,8}O_{1,9}$ phase with fluorite structure. In the sintered powder made after 450 W sonochemical

treatment, only $Eu_2Zr_2O_7$ reflections with a pyrochlore structure are present. On the basis of the performed tests, it can be concluded that the use of sonochemistry in the homogenization of powder has a positive effect on sintering and makes it possible to obtain a pyrochlore structure.

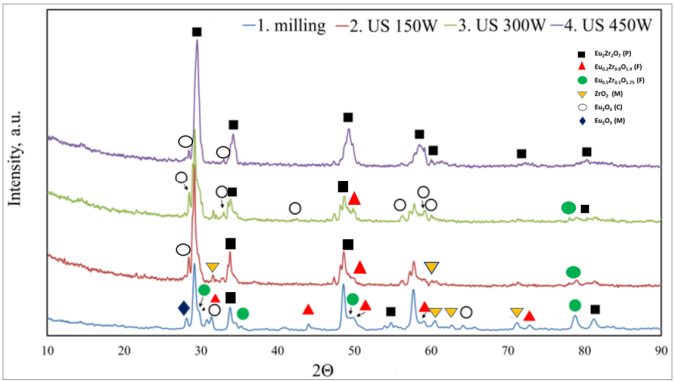

Fig. 8. XRD patterns after sintering of differently homogenized powder mixtures

4. Summary

Sonochemical method of powders homogenization changed the particle size distribution of ZrO_2-Eu_2O_3 powder mixtures. Range of particle size moved to lower values, whereas occurred additional agglomeration. Ultrasound processing did not change the phase composition and morphology of investigated powder mixtures. Thermal analysis of ZrO_2-Eu_2O_3 showed substantial differences in powders after homogenized using different power densities of sonochemical treatment, however, did not reveal clear peaks corresponding to synthesis. DSC curves after different variants of homogenizing were similar.

Sonochemical method of homogenization is relatively new for this type of ceramics, therefore this method should be evaluated for other compounds (e.g. cerates, hafnates). Moreover, there is a need to understand the role of applied power density in homogenization and how it may be tailored in order to obtain the most homogeneous and beneficial mixtures.

Acknowledgements

We gratefully acknowledge the financial support of the National Science Centre, Poland under grant number 2016/21/D/ST8/01687.

REFERENCES

[1] Jeanine T. DeMasi-Marcin, Dinesh K. Gupta, Protective coatings in the gas turbine engine, Surface and Coatings Technology **68-69**, 1-9 (1994).

[2] D.R. Clarke, M. Oechsner, N.P. Padture, Thermal-barrier coatings for more efficient gas-turbine engines, MRS Bulletin **37** (10), 891-898 (2012).

[3] D.R. Clarke, S.R. Phillpot, Thermal barrier coating materials, Materials Today **8** (6), 22-29 (2005).

[4] R. Vassen, M.O. Jarligo, T. Steinke, D.E. Mack, D. Stöver, Overview on advanced thermal barrier coatings, Surface and Coatings Technology 205 (4), 938-942 (2010).

[5] F.H Stott, D.J. Wet, R. de Taylor, Degradation of thermal-barrier coatings at very high temperatures, MRS Bulletin **19** (10), 46 (1994).

[6] J.L. Smialek, F.A. Archer, R.G. Garlick, Turbine airfoil degradation in the Persian Gulf war, JOM **46** (12), 39-41 (1994).

[7] M.P. Borom, C.A. Johnson, L.A. Peluso, Role of environmental deposits and operating surface temperature in spallation of air plasma sprayed thermal barrier coatings, Surface and Coatings Technology **86-87** (1), 116 (1996).

[8] J. Kim, M.G. Dunn, A.J. Baran, D.P. Wade, E.L. Tremba, Deposition of volcanic materials in the hot sections of two gas turbine engines, J. Eng. Gas Turbines Power **115** (3), 641 (1993).

[9] C. Mercer, S. Faulhaber, A.G. Evans, R. Darolia, A delamination mechanism for thermal barrier coatings subject to calcium-magnesium-alumino-silicate (CMAS) infiltration Acta Materialia **53** (4), 1029-1039 (2005).

[10] S. Krämer, S. Faulhaber, M. Chambers, D.R. Clarke, C.G. Levi, J.W. Hutchinson, A.G. Evans, Mechanisms of cracking and delamination within thick thermal barrier systems in aero-engines subject to calcium-magnesium-alumino-silicate (CMAS) penetration, Materials Science and Engineering A **490** (1-2), 26-35 (2008).

[11] R.L. Jones, Some aspects of the hot corrosion of thermal barrier coatings, Journal of Thermal Spray Technology **6** (1), 77-84 (1997).

[12] N.Q. Wu, Z. Chen, S.X. Mao, Hot corrosion mechanism of composite alumina/yttria-stabilized zirconia coating in molten sulfate-vanadate salt, Journal of the American Ceramic Society **88** (3), 675-682 (2005).

[13] B.R. Marple, J. Voyer, C. Moreau, D.R. Nagy, Corrosion of Thermal Barrier Coatings by Vanadium and Sulfur Compounds, Materials at High Temperature **17** (3), 397-412 (2000).

[14] A. Zhang, M. Lü, G. Zhou, S. Wang, Y. Zhou, Combustion synthesis and photoluminescence of Eu3+, Dy3+-doped La2Zr2O7 nanocrystals, Journal of Physics and Chemistry of Solids **67** (11), 2430-2434 (2006).

[15] J.Y. Li, H. Dai, Q. Li, X.H. Zhong, X.F Ma, J. Meng, X.Q. Cao, Lanthanum zirconate nanofibers with high sintering-resistance, Materials Science and Engineering B **133** (1-3), 209-212 (2006).

[16] B.D. Begg, N.J. Hess, D.E. McCready, S. Thevuthasan, W.J. Weber, Heavy-ion irradiation effects in Gd2(Ti2-xZrx)O7 pyrochlores, Journal of Nuclear Materials **289** (1-2), 188-193 (2001).

[17] C.R. Stanek, Atomic Scale Disorder in Fluorite and Fluorite Related Oxides. PhD Thesis, Imperial College of Science, Technology and Medicine. London SW7 2AZ, August 2003.

[18] K.S. Suslick, D.A. Hammerton, R.E. Cline Jr., J. Am. Chem. Soc. 108, 5641-5642 (1986).

[19] B. Toukoniitty, J.-P. Mikkola, D.Yu. Murzin, T. Salmi, Applied Catalysis A 279, 1-22 (2005).